Supporting Information

Carbon Coated Bimetallic Sulfide Nanodots/Carbon Nanorod Heterostructure Enabling Long-life Lithium- ion Batteries

Xuejie Gao, [a] *Jiwei Wang*[b], *Duo Zhang,* [c] *Keegan Adair*[b], *Kun Feng,*[a] *Na Sun,* [a] *Hechuang Zheng,* [a] *Huiyun Shao,* [a] *Jun Zhong,* [a] *Yanyun Ma,*[a,]* *Xueliang (Andy) Sun*[b,]* *and Xuhui Sun*[a,]*

a. Institute of Functional Nano and Soft Materials (FUNSOM), Jiangsu Key Laboratory for Carbon-Based Functional Materials and Devices, and Collaborative Innovation Center of Suzhou Nano Science and Technology, Soochow University, Suzhou 215123, China

b. Department of Mechanical and Materials Engineering, University of Western Ontario, London, Ontario, N6A 5B8, Canada.

c. School for Radiological and Interdisciplinary Sciences (RAD-X), Soochow University, Suzhou 215123, China.

*Corresponding Author: mayanyun@suda.edu.cn, xsun9@uwo.ca, xhsun@suda.edu.cn.

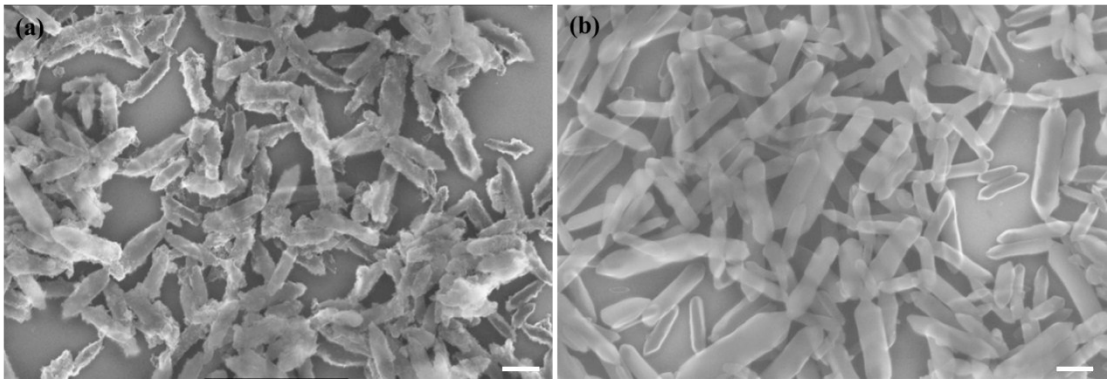

Figure S1. SEM image of CH_4N_2S@Fe_2Ni MIL-88 before (a) and after coating glucose (b). Scale bar: 200 nm.

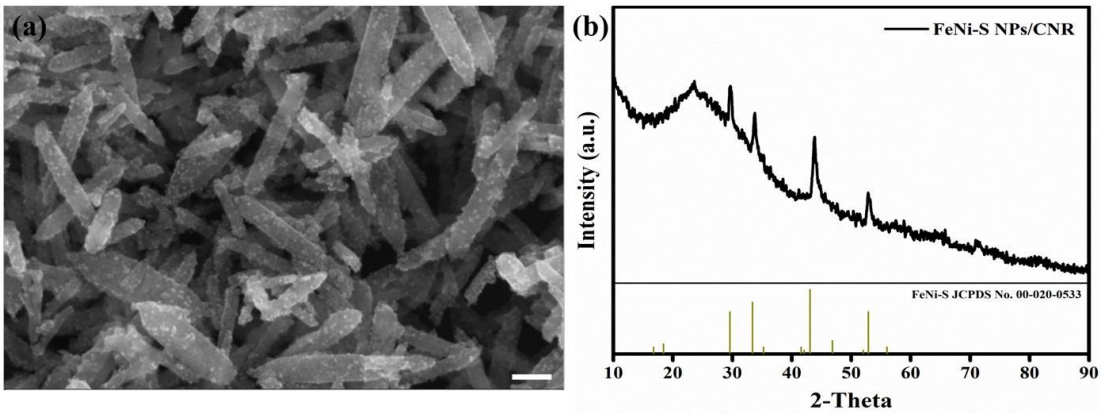

Figure S2. SEM image of FeNi-S NPs/CNR (a) and the corresponding XRD pattern. (b). Scale bar: 200 nm.

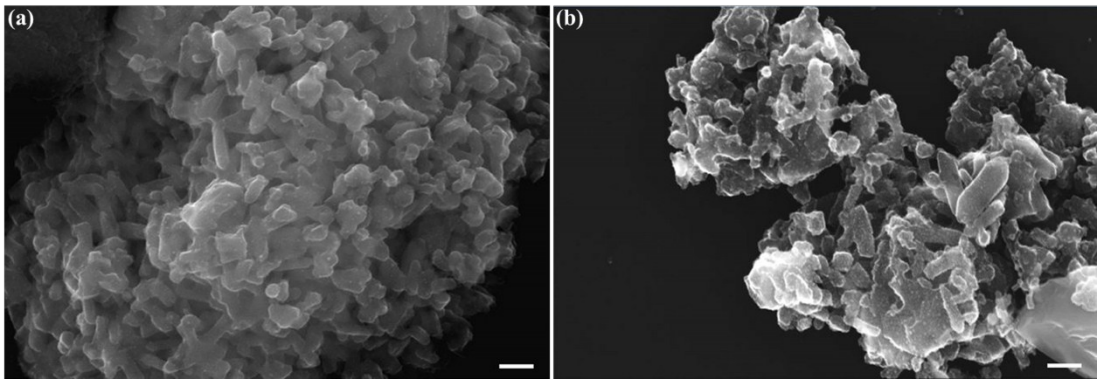

Figure S3. SEM images of the products obtained after annealing of the glucose wrapped CH_4N_2S@Fe_2Ni MIL-88 nanorods at 600 ℃ for different time: (a) 1 h and (b) 3h. Scale bar: 200 nm.

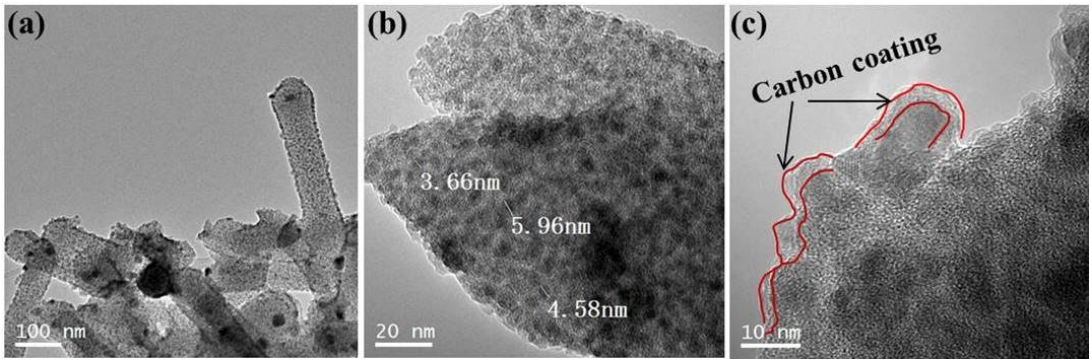

Figure S4. TEM images of C@FeNi-S NDs/CNR with different magnifications.

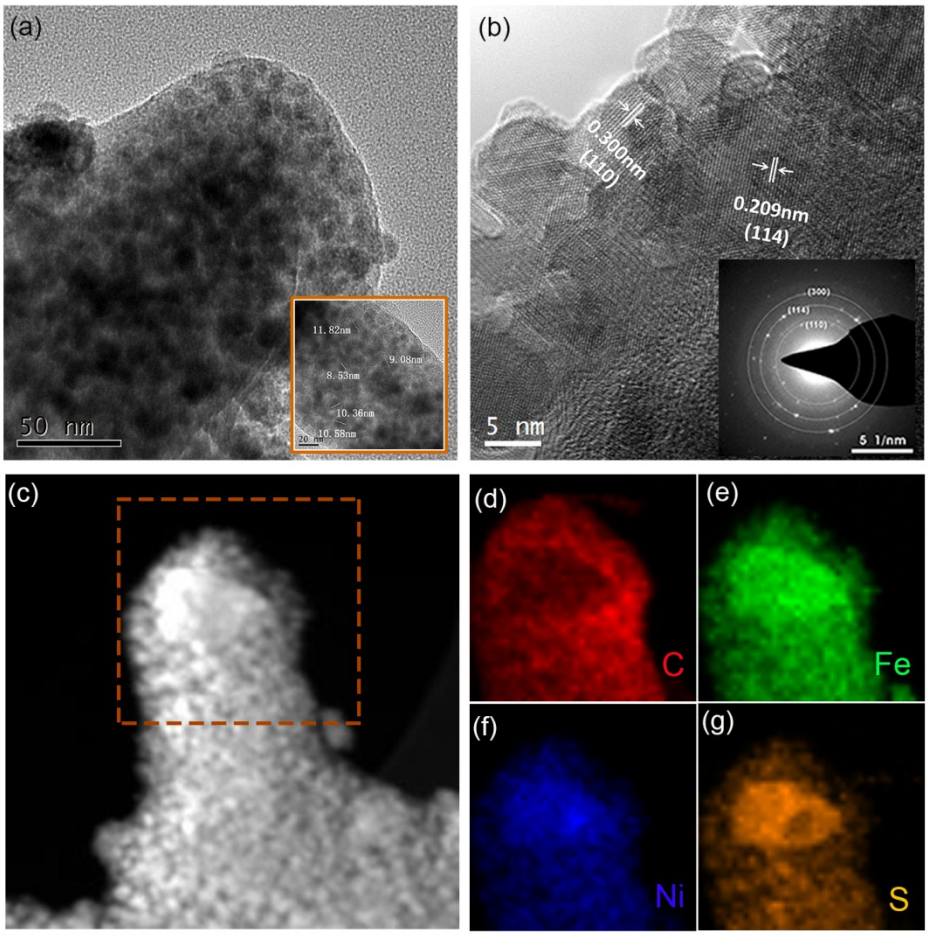

Figure S5. TEM image (a), HRTEM image and indexed SAED pattern (insert) (b), and elemental mapping images (c-g) of FeNi-S NPs/CNR.

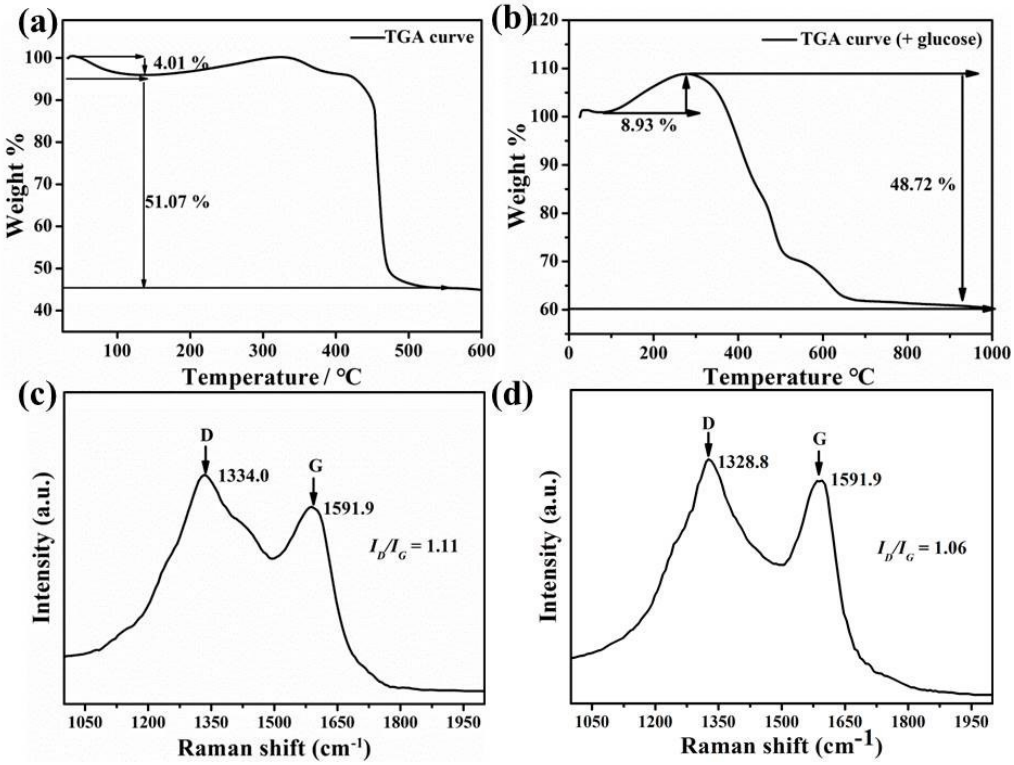

Figure S6. (a) and (c) are TGA curve and Raman spectra of C@FeNi-S NDs/CNR, (b) and (d) are TGA and Raman spectra of FeNi-S NPs/CNR.

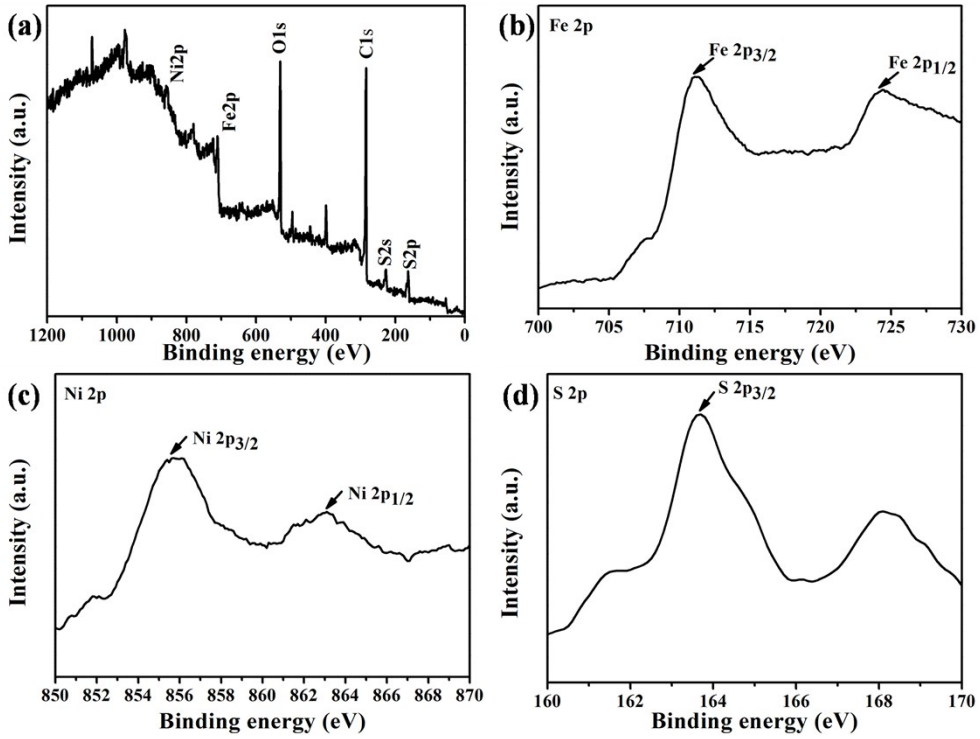

Figure S7. XPS spectra of C@FeNi-S NDs/CNR: survey scanned XPS spectrum (a) and high-resolution XPS spectra for (b) Fe 2p, (c) Ni 2p and (d) S 2p.

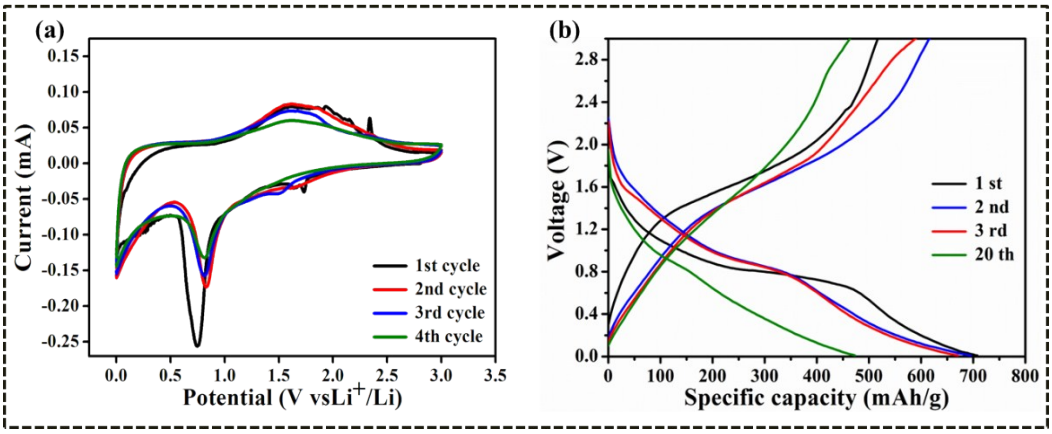

Figure S8. (a) CV curves at a scan rate of 0.1 mV/s for the initial four cycles of FeNi-S NPs/CNR; (b) Galvanostatic charge-discharge voltage profiles for the different cycles at a rate of 0.5 C for FeNi-S NPs/CNR. Voltage range: 0.01-3.0 V vs. Li/Li^+.

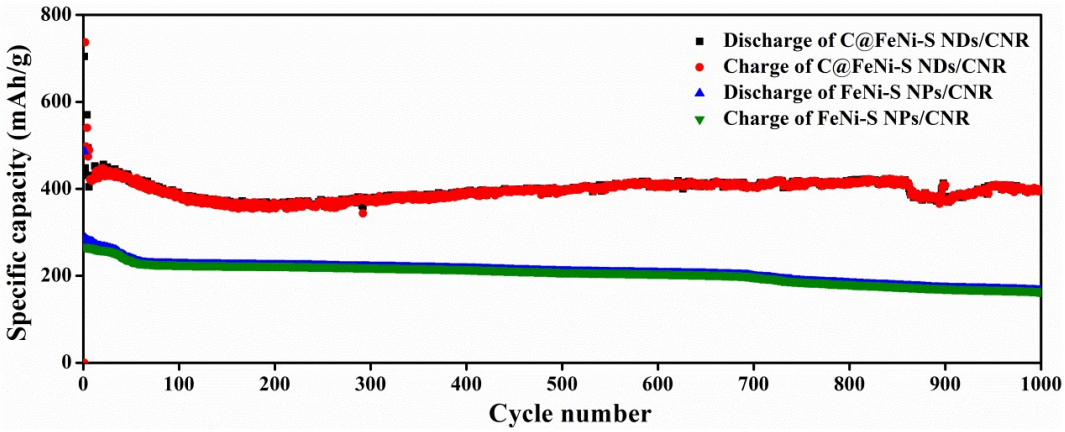

Figure S9. Capacity retention of C@FeNi-S NDs/CNR and FeNi-S NPs/CNR at a rate of 6 C for 1000 cycles.

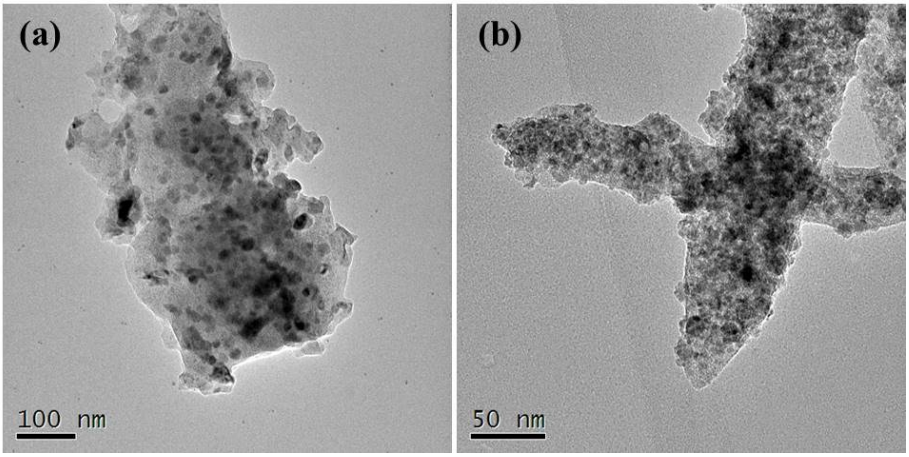

Figure S10. TEM images of FeNi NPs/CNR and C@FeNi NDs/CNR (a) and (b), after 200 cycles at 0.5 C.

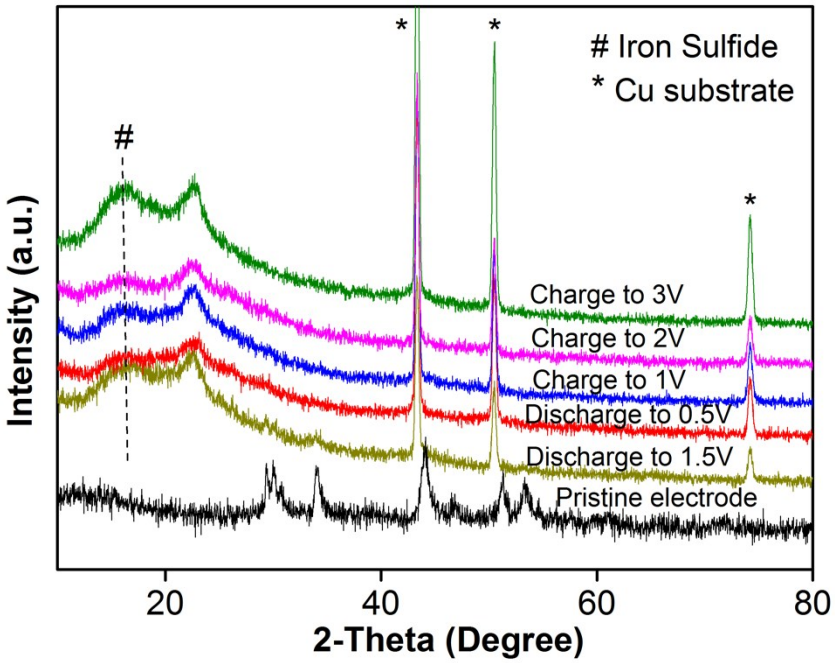

Figure S11. XRD patterns of of C @ FeNi-S NDs/CNR electrodes at various discharge/charge voltages.

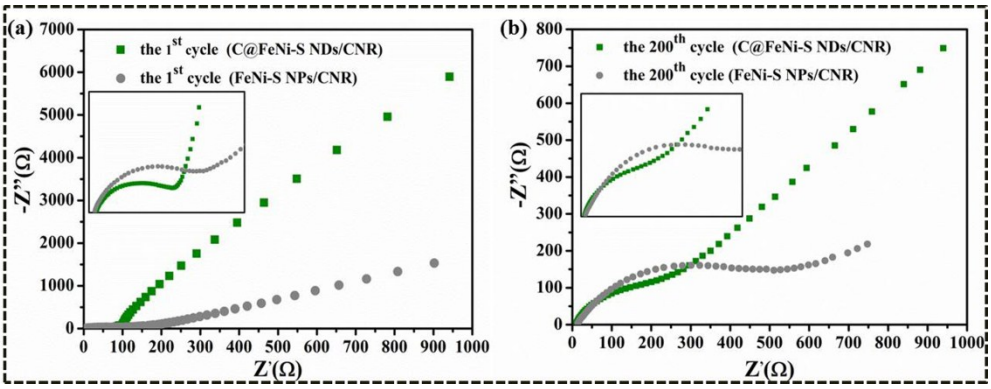

Figure S12. Nyquist plots for comparison of C@FeNi-S NDs/CNR and FeNi-S NPs/CNR at the 1st cycle (a) and the 200th cycle (b) in frequency range of 0.01–10^5 Hz.

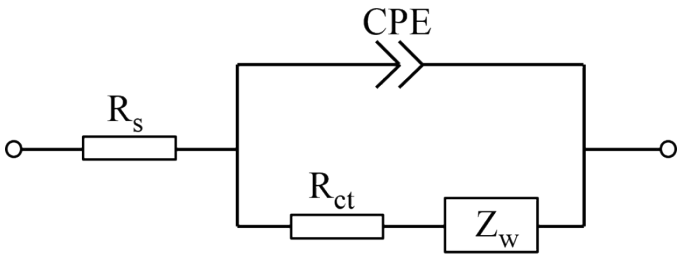

Figure S13. Equivalent circuit for EIS results fitting.

Table S1. Summary of cycling performance for TMS-based anodes in LIBs.

TMS based anode	**Current density/ rate**	**Cycle number**	**Specific capacity (mAh/g)**	**Ref.**
$NiCo_2S_4/Ni_{0.96}S$ on graphene	100 mA/g	200	965	1
$NiCo_2S_4$ on Nickel foam	0.2C	50	720	2
$Fe_{1-x}S$/C nanocomposites	100 mA/g	200	1185	3
Coated/Sandwiched rGO/CoSx composites	100 mA/g	100	613/670	4
FeS_2 Decorated Sulfur-doped Carbon	100 mA/g	100	689	5
Fiber (FeS2@S-C)	1000 mA/g	150	500	
transition metal sulfide	100 mA/g	350	550	

nanoparticles embedded in carbon matrices ①FeS@C nanocomposites	500 mA/g	500	480	6
②Ni_2S@C nanocomposites	100 mA/g	160	670	
Ni_3S_4/NG-250°C composite	0.2 C	100	1323.2	7
Graphene-wrapped nickel sulfide nanoprisms	70 mA/g	100	1200	8
FeS@C-N hierarchical porous microspheres	100 mA/g	100	983.5	9
FeS/porous carbon composite	0.1 C	150	624.9	10
C@FeNi-S NDs/CNR	**0.5C**	**200**	**851.3**	**This work**
	4C	**1000**	**484.7**	
	6C	**1000**	**361.0**	

Reference

1. D. Bai, F. Wang, J. Lv, F. Zhang and S. Xu, *ACS applied materials & interfaces*, 2016, 8, 32853-32861.
2. D. J. Yu, Y. F. Yuan, D. Zhang, S. M. Yin, J. X. Lin, Z. Rong, J. L. Yang, Y. B. Chen and S. Y. Guo, *Electrochimica Acta*, 2016, 198, 280-286.
3. C. Wang, M. Lan, Y. Zhang, H. Bian, M.-F. Yuen, K. Ostrikov, J. Jiang, W. Zhang, Y. Y. Li and J. Lu, *Green Chem.*, 2016, 18, 3029-3039.
4. D. Yin, G. Huang, F. Zhang, Y. Qin, Z. Na, Y. Wu and L. Wang, *Chemistry*, 2016, 22, 1467-1474.
5. Y. Gan, F. Xu, J. Luo, H. Yuan, C. Jin, L. Zhang, C. Fang, O. Sheng, H. Huang, Y. Xia, C. Liang, J. Zhang, W. Zhang and X. Tao, *Electrochimica Acta*, 2016, 209, 201-209.
6. P. Lou, Y. Tan, P. Lu, Z. Cui and X. Guo, *J. Mater. Chem. A*, 2016, 4, 16849-16855.
7. N. Mahmood, C. Zhang and Y. Hou, *Small*, 2013, 9, 1321-1328.
8. A. A. AbdelHamid, X. Yang, J. Yang, X. Chen and J. Y. Ying, *Nano Energy*, 2016, 26, 425-437.
9. Z.-G. Wu, J.-T. Li, Y.-J. Zhong, J. Liu, K. Wang, X.-D. Guo, L. Huang, B.-H. Zhong and S.-G. Sun, *Journal of Alloys and Compounds*, 2016, 688, 790-797.
10. S.-P. Guo, J.-C. Li, Z. Ma, Y. Chi and H.-G. Xue, *Journal of Materials Science*, 2016, 52, 2345-2355.